NUMERICAL SIMULATIONS OF BURSTY PLANETARY RADIO EMISSIONS

R. M. Winglee*, J. D. Menietti*, and H. K. Wong*

Abstract

The Voyager spacecraft observed both smooth and bursty radio emissions from Uranus and Neptune. These emissions are known to be freely propagating primarily in the right hand circularly polarized mode (RCP) with the bursty emissions having burst periods as short as a few tenths of a second and the smooth emissions being observed over periods of a few hours. While the smooth emission is probably due to the electron cyclotron maser instability some other processes must be at work to produce the bursty emissions. It is proposed that one important difference in mechanisms is that the smooth emissions are associated with continuous injection of electrons while the bursty emissions are associated with impulsive injection. In the latter case, the electron distribution can develop a beam feature with a temperature anisotropy which is unstable to an electromagnetic beam instability that can generate bursty emissions. The characteristics of this radiation is determined via one dimensional (three velocity) particle simulations. It is shown that the electromagnetic beam instability anisotropy is as efficient as the maser instability in converting particle energy to wave energy. For $\omega_{pe}/\Omega_e \gtrsim 1$, most of the wave energy is LCP but is trapped. However, for $\omega_{pe}/\Omega_e \lesssim 1$ the dominant mode is RCP and freely propagating. Furthermore, the radiation is bursty in nature due to the competition between different modes and is most intense when $0.4 \lesssim \omega_{pe}/\Omega_e \lesssim 1$. This regime complements that of the maser emission which is expected to be most intense when $\omega_{pe}/\Omega_e \lesssim 0.3$.

1 Introduction

Observations of planetary radio emissions from Uranus and Neptune obtained by the Voyager 2 spacecraft have shown clear evidence of two distinct classes of radiation characterized as smooth and bursty. At Uranus, the smooth emission is seen as broadband continuous emissions, from a few kilohertz to about 900 kHz and continuous in time over periods of a few hours. Many studies have suggested the b–smooth emission is generated by the cyclotron–maser instability [e.g. Kaiser et al., 1987; Menietti et al., 1990].

*Department of Space Sciences, Southwest Research Institute, San Antonio, TX 78228–0510

The Uranian broadband bursty (b–bursty) emission is seen in the range from 300–700 kHz and occurs at times which are intermediate between the observations of the smooth emissions (see Plate 1 of Farrell and Calvert [1989] for an excellent graphical display). Thus, the smooth and bursty emissions are quite distinct in frequency range, duration and spacecraft event time.

Many early studies based on straight–line propagation [cf. Leblanc et al., 1987 and Farrell and Calvert, 1989] indicated the source of the b–bursty emission was co–located with the smooth emission near the south magnetic pole. These early studies generally agree that the emission propagates at large wave normal angles and suggest the cyclotron maser instability (CMI) as the source mechanism. However, Curran et al. [1990] have shown, via a ray tracing study, that refractive effects are important and that the source of the bursty emissions appears to be at lower latitudes for emission initially propagating at large wave normal angles. The conclusion of this latter study was that since the source region is different from that of the b–smooth emission, it is possible that the emission may be due to a distinct plasma distribution at lower latitudes or a source mechanism that is different from that which generates the b–smooth emission.

Observations of the radio emission obtained by the Voyager 2 flyby of Neptune also show clear examples of both a bursty and a smooth component [e.g. Warwick et al., 1989; Farrell et al., 1990]. The bursty emission is observed between 500 kHz and 1.3 MHz while the smooth emission is seen in the frequency range $f < 500$ kHz. The bursty emission is also generally observed at distinct times from the smooth emission and their source regions appear to be different [Farrell et al., 1990; Ladreiter et al., 1991]. The emission appears to occur in episodes with strong bursts of duration < 6 seconds, and the polarization is consistent with the right–hand extraordinary mode. Generally the bandwidth of the Neptune bursty emission is much shorter than the b–bursty emission at Uranus, with the former having a bandwidth of less than 20 kHz.

It has been suggested that both the smooth and bursty emissions are due to the electron cyclotron emissions, similar to the proposal for the emissions at Uranus [e.g., Farrell et al., 1990 and references therein]. However, the above differences in the characteristics of the smooth and bursty emissions suggest that either there are distinct emission mechanisms at work and/or that there are distinct differences in the plasma conditions in the source region.

Recently Wong and Goldstein [1990] suggested a new mechanism for producing bursty radio emission under conditions expected in planetary magnetospheres using temperature anisotropic electron beams. This mechanism was originally proposed by Goldman and Newman [1987] to explain a 'new electromagnetic beam mode' discovered in laboratory experiments reported by Urrutia and Stenzel [1984]. The mechanism suggests that a gyrating electron beam or an electron beam with a temperature anisotropy of the form $T_\perp \gg T_\parallel$ can directly generate EM radiation through a cyclotron resonant–wave–particle interaction. Newman et al. [1988] subsequently performed a comprehensive study of the mechanism including numerical simulations for the case when the ratio of the plasma frequency (ω_{pe}) to gyrofrequency (Ω_e) was greater than 2. Wong and Goldstein [1990] have extended the theory to the region of $\omega_{pe}/\Omega_e \lesssim 1$ typical of planetary magnetospheres. Their results suggest that this mechanism, hereafter called the electromagnetic beam

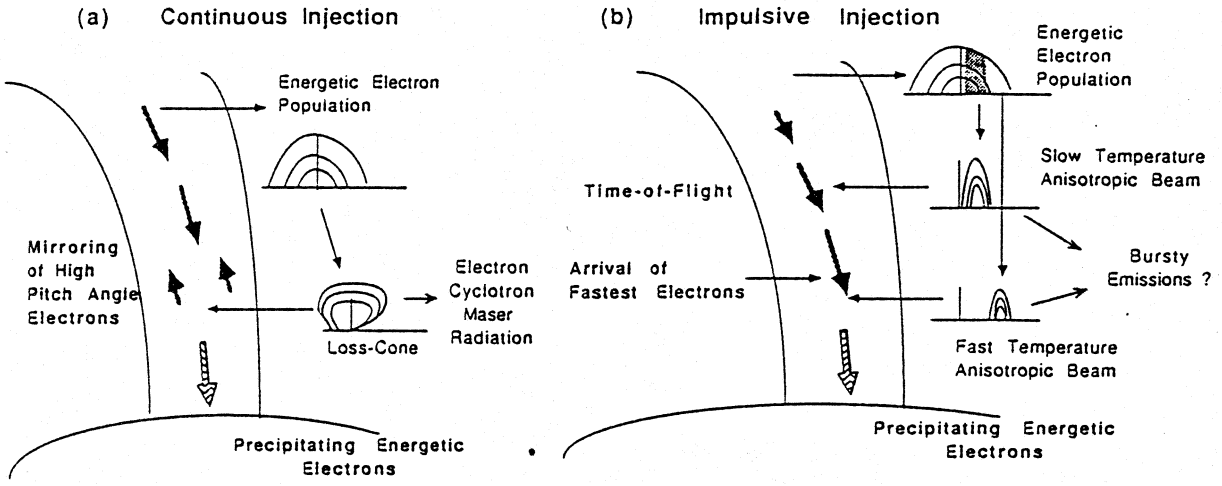

Figure 1: Schematic showing (a) the development of a loss–cone distribution during continuous injection of energetic electrons and the subsequent generation of maser emission responsible for the smooth emissions and (b) the development of a temperature anisotropic beam during impulsive injection. This type of beam can drive a modified Weibel instability which can generate radiation which can possibly account for the bursty emissions.

instability (EBI), can easily generate radiation as much as a factor of two above the electron cyclotron frequency, the radiation being beamed into a filled emission cone of half–angle less than 30°.

In this paper one–dimensional particle–in–cell simulations are used to investigate the radiation from electron beams with a large temperature anisotropy. It is shown that these beams, which would typically orginate from the sporadic or impulsive injection of energetic electrons, can generate electromagnetic radiation which should be able to escape into the solar wind when the ratio of the electron plasma frequency ω_{pe} to the electron cyclotron frequency Ω_e is between about 0.4 to 1.0. Moreover, this parameter regime complements that required for the maser instability which tends to be restricted to $\omega_{pe}/\Omega_e \lesssim 0.3$ and thereby provides a natural explanation for the apparent differences in source location and spacecraft event times between the smooth and bursty emissions.

2 Comparison between maser and beam instabilities

The processes which may be involved in the generation of both the smooth and bursty emissions are illustrated in Figure 1. The standard model for producing the smooth emissions is shown in Figure 1a. Because of the long duration of the smooth emissions, there must be a continual resupply of the energetic electrons producing the radiation otherwise the driving mechanism would quickly saturate and the emissions would cease. For such a continual flow of energetic electrons down the field lines, a loss cone distribution would form, as electrons with high pitch angles mirror and move back up the field lines, while electrons with small pitch angles precipitate out of the flux tube and are lost to the lower atmosphere. Such loss–cone distributions are unstable to the maser instability which generates the observed radiation for the smooth emissions.

For the bursty emissions, the physics involved is substantially different. In particular, the presence of short bursts implies that the energetic electrons responsible for the emissions are being injected intermittently. For rapid or impulsive injection, only certain particles can reach a point further down the field line at any particular time, since slow particles would not have had sufficient time to reach it and fast particles would have already passed by [e.g., White et al., 1986; Winglee and Dulk, 1986]. As a result of these time–of–flight effects, the distribution locally can be narrowly confined in the parallel velocity, allowing the distribution to develop a beam–like feature. Furthermore, since the time–of–flight effects depend only weakly on the perpendicular velocity (assuming only weak magnetic field convergence), the particles arriving at any particular point can have a much larger spread in the perpendicular velocity than in their parallel velocity, effectively giving the beam a temperature anisotropy as well. Note that these types of distributions can develop from the same initial distribution as that driving the loss–cone formation; the main differences in the evolution of the distribution arise from the duration over which the particles are injected.

These temperature anisotropic beams are unstable to a modified kinetic 'Weibel instability' or electromagnetic beam instability [Newman et al., 1988]. When the ratio of the plasma frequency ω_{pe} to the electron cyclotron frequency Ω_e is much greater than one, modified whistlers are excited [Newman et al., 1988]. However, if $\omega_{pe}/\Omega_e < 1$, then Wong and Goldstein [1990] predict that the dominant emission is in the RCP X–mode with $\omega > \Omega_e$ and it is this radiation which they propose as the possible source of the bursty planetary emissions. In the following, the non–linear evolution of the instability is examined through particle simulations in order to compare the characteristics of the radiation with that from the maser instability and, thereby, provide better insight into the possible origins of the bursty and smooth emissions.

3 Particle distributions and particle heating

The non–linear evolution of the electromagnetic beam instability is investigated via one–dimensional (three velocity) electromagnetic particle simulations [cf. Newman et al., 1988]. This code solves self–consistently the full set of Maxwell's equations and allows the evaluation of the competition between electromagnetic and electrostatic beam instabilities. The system is assumed to be periodic with the wavevector k directed along the magnetic field which is in the X–direction. The size of the system L is assumed to be 1024 Debye lengths and the corresponding wavenumber of a mode m in the system is then $2\pi m/L$.

In all the following simulations the density of the plasma is kept constant and the magnetic field strength is varied so that ω_{pe}/Ω_e ranges from a maximum value of 2.5 down to a minimum value of 0.4. This parameter regime extends that considered by Newman et al. [1988] where only values of $\omega_{pe}/\Omega_e \geq 2.5$ were considered.

The plasma is assumed to consist of (i) a cold ambient plasma with a Maxwellian distribution with thermal speed v_{Tc} equal to $0.04c$ and which comprises 90% of the total electron density and (ii) a beam component with a beam speed v_b equal to $4v_{Tc}$, a parallel

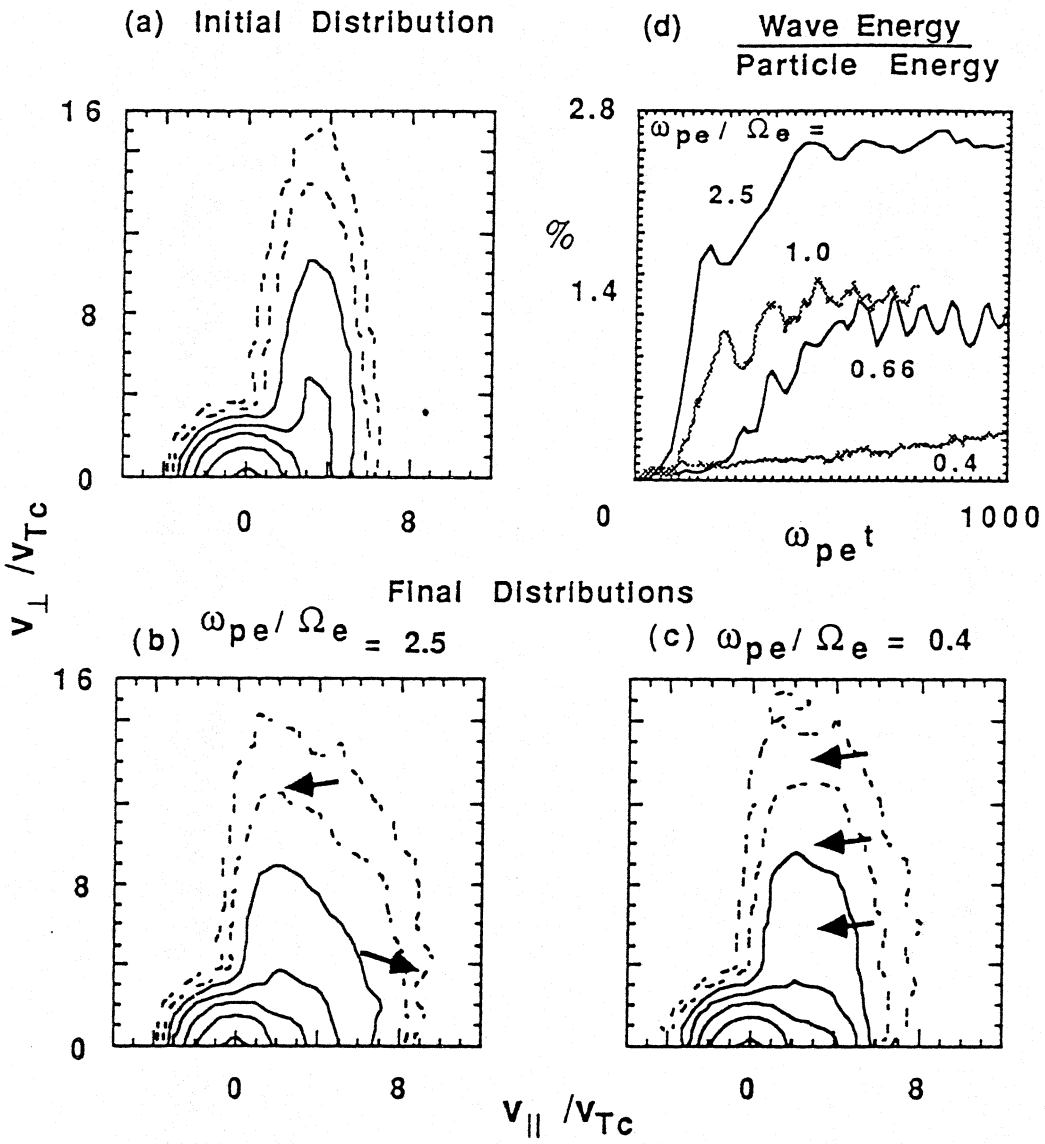

Figure 2: Evolution of the total electron distribution. The initial distribution is shown in (a) and the final distributions at saturation are shown in (b) and (c) for ω_{pe}/Ω_e equal to 2.5 and 0.4, respectively. The time history of the percentage of the particle energy converted to wave energy is shown in (d).

temperature the same as the cold component and a perpendicular temperature 36 times the parallel temperature, i.e $v_{T\|E} = v_{Tc}, v_{T\perp E} = 6v_{T\|E}$. These parameters are similar to those used by Newman et al. [1988].

The initial distribution comprising these two components is shown in Figure 2a. It is unstable to both the electromagnetic beam instability as well as a weak electrostatic beam instability (similar to the normal bump–in–tail instability). The electrostatic instability quickly saturates (by $\omega_{pe}t \simeq 100$) and produces only some flattening of the distribution between $3 \lesssim v_\|/v_{Tc} \lesssim 4$. Most of the particle heating is driven by the electromagnetic beam instability, as illustrated in Figures 2b and c which show the velocity distributions at saturation ($\omega_{pe}t \simeq 1000$) for the extreme values of ω_{pe}/Ω_e considered.

For $\omega_{pe}/\Omega_e \gtrsim 1$ (Figure 2b), the electromagnetic beam instability scatters low pitch angle electrons forward to higher $v_\parallel$ and high pitch angle electrons to lower pitch angles and lower energies. For $\omega_{pe}/\Omega_e \lesssim 1$, the beam particles experience primarily only scattering to lower pitch angles and energies. The fraction of particle energy converted to wave energy is shown in Figure 2d. The efficiency is seen to increase with increasing ω_{pe}/Ω_e even though the instability at high ω_{pe}/Ω_e is associated with acceleration of some of the particles to higher $v_\parallel$. This increase in efficiency is consistent with the increase in the expected growth rate of the instability as ω_{pe}/Ω_e is increased for a fixed energetic component [cf. Wong and Goldstein, 1990]. It should also be noted that the efficiency of the instability is comparable to that of the maser instability [e.g., Pritchett, 1986], i.e. the electromagnetic beam instability can, under certain conditions, produce radiation as intense as the maser instability.

4 Characteristics of the wave spectrum

The characteristics of the excited waves are expected to change as ω_{pe}/Ω_e is varied from above to below unity. In particular, for $\omega_{pe}/\Omega_e \gtrsim 1$ the whistler, through a Doppler shift associated with the presence of the beam, can have a frequency comparable to the electron cyclotron frequency, allowing gyro–resonant interactions to occur. However, when $\omega_{pe}/\Omega_e \lesssim 1$, the maximum frequency of the whistler is limited to ω_{pe} where it becomes increasingly electrostatic so that gyroresonant interactions are suppressed. However, the cutoff for the X–mode and resonance for the Z–mode start to approach the cyclotron frequency and it is these modes which can then become unstable through gyro–resonant interactions.

This change in the mode structure is illustrated in Figure 3 which shows the spectrum derived from integrating the power in the different k modes over the full period of the simulations. It is seen that, for $\omega_{pe}/\Omega_e = 2.5$, the dominant emission is at about 0.5 Ω_e and is left hand polarized (LCP). This mode is essentially a beam–modified backward propagating whistler. Because its frequency is below Ω_e this emission is expected to be trapped in a planetary magnetosphere.

At the intermediate values of ω_{pe}/Ω_e (Figures 3b and c), there is still relatively strong emission at 0.5 Ω_e. In addition, strong emissions at frequencies slightly above Ω_e appear. This is the RCP X–mode predicted by Wong and Goldstein [1990] and it is this radiation, particularly for the lower values of ω_{pe}/Ω_e, which can escape into the solar wind and produce the bursty emissions. Since this is the only component that can escape, the observed radiation should be highly polarized similar to the radiation from the maser instability. At still lower values of ω_{pe}/Ω_e (Figures 3d), the LCP emission is essentially suppressed and the emission in the RCP Z–mode at frequencies fractionally below the Ω_e becomes increasingly stronger.

In addition to the above variations in the overall spectrum of the generated radiation, there are also significant changes in the temporal evolution of the dominant modes as ω_{pe}/Ω_e is varied. As an example, Figure 4 shows the time histories of the power of the dominant modes for ω_{pe}/Ω_e equal to (i) 1.0 and (ii) 0.4. For the higher value of ω_{pe}/Ω_e the modes

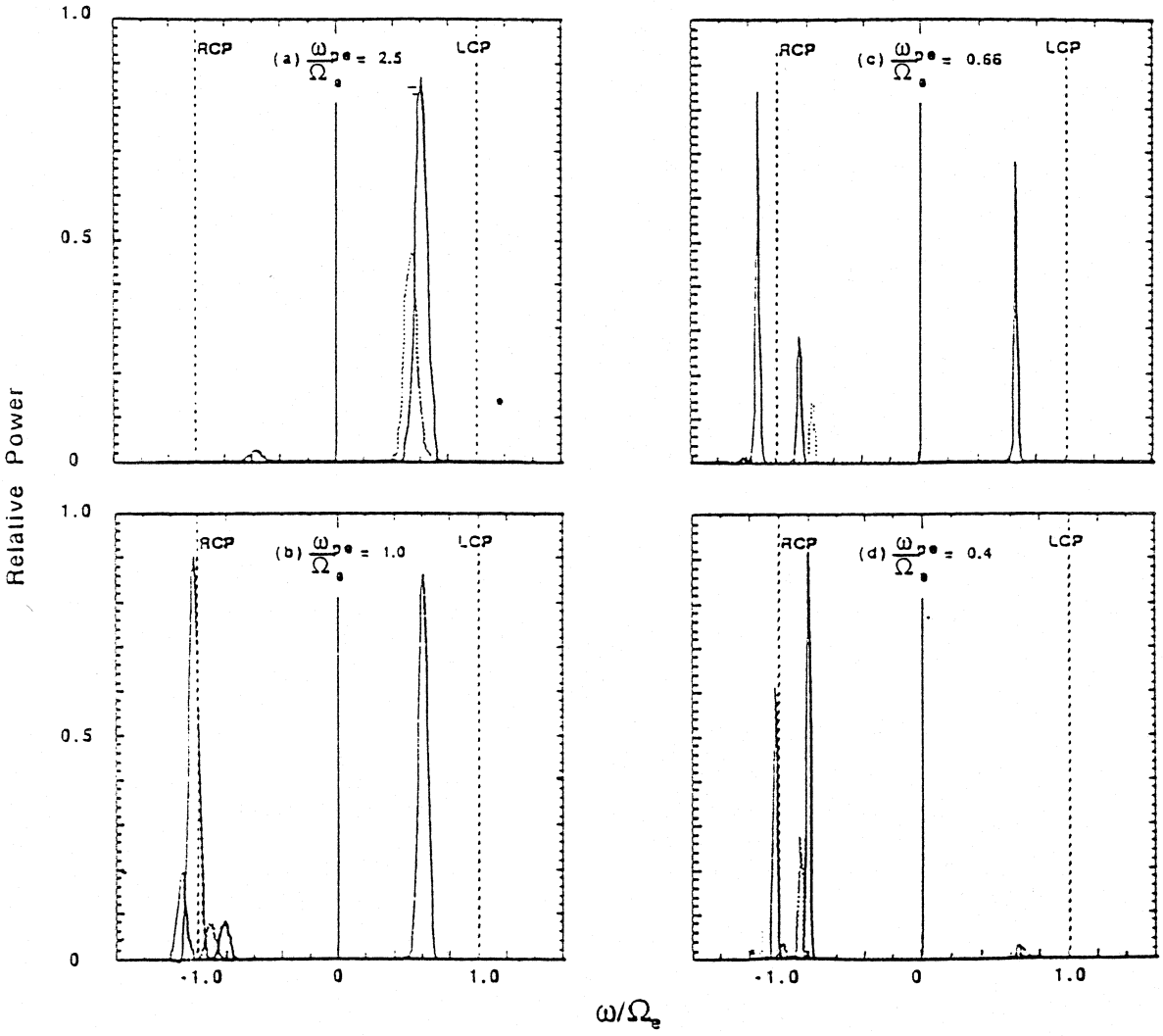

Figure 3: Power spectra of the dominant modes for the cases shown in Figure 3. The spectra have been normalized so that the spectral peak has approximately the same value in each case. For the highest value of ω_{pe}/Ω_e, the LCP mode with $\omega \simeq 0.5\Omega_e$ dominates but as ω_{pe}/Ω_e is decreased the RCP modes dominate, with intense emissions above Ω_e being generated.

grow approximately monotonically up to their peak value and then stay approximately constant, with possibly a small, slow decay. This type of temporal evolution is similar to that of the maser instability and would be probably more closely associated with long duration bursts.

For the smaller value of ω_{pe}/Ω_e (right hand side of Figure 4), the temporal evolution of the dominant mode is significantly different. Instead of a monotonic rise, the amplitude of the modes is seen to reach a series of local maxima. These temporal variations are due to the competition between the modes for the available free energy. In particular, the maxima and minima of the two modes shown are approximately anti–correlated. As a result of this competition, the radiation in this parameter regime is intrinsically bursty.

The growth rates for the different modes can be directly calculated from the time histories

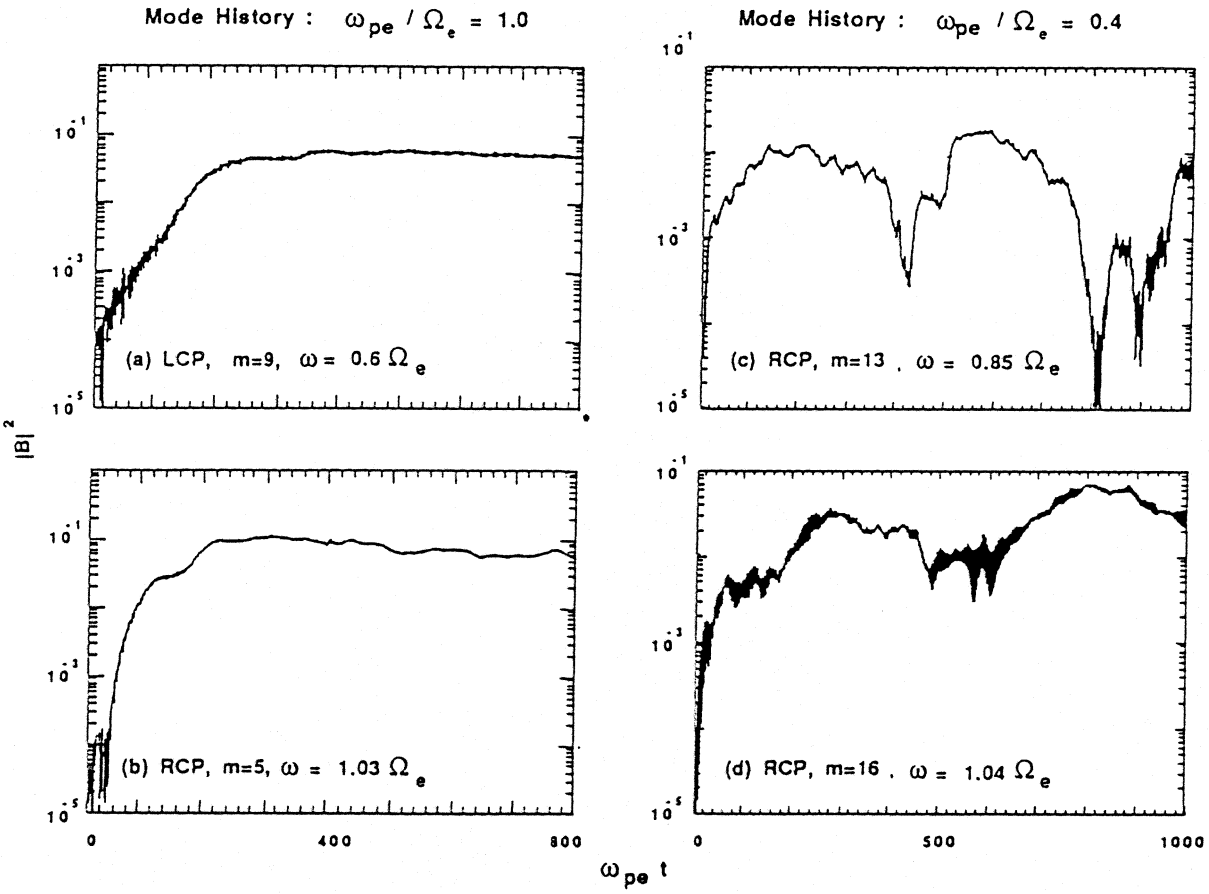

Figure 4: Time histories of the power in dominant modes for ω_{pe}/Ω_e equal to 1.0 (left hand side) and 0.4 (right hand side). At the lower value of ω_{pe}/Ω_e, the emissions are bursty due to competition modes.

shown in Figure 4. For $\omega_{pe}/\Omega_e = 1.0$ (Figure 4a), the growth rate of the LCP mode is about 0.02 Ω_e and between about 0.02 and 0.04 Ω_e for the RCP mode. For $\omega_{pe}/\Omega_e = 0.4$, the growth rate is smaller being about 2–4$\times 10^{-3}$ Ω_e. These growth rates are consistent with the linear growth rates predicted by Wong and Goldstein [1990] and are comparable to those for the maser instability.

5 Conclusions

One–dimensional electromagnetic particle simulations have been used to evaluate the characteristics of radiation from electron beams with temperature anisotropies in order to identify the origin of bursty planetary emissions. Such beams can arise for example during the impulsive injection of energetic electrons with time–of–flight effects restricting the parallel velocity of the particles arriving at any particular point down the field lines at a specific time. Observations of temperature anisotropies and electron beams in the Earth's auroral region have recently been reported for terrestrial observations [cf. Menietti and Burch, 1991]. These observations indicate that temperature anisotropies ($T_\perp \gg T_\parallel$)

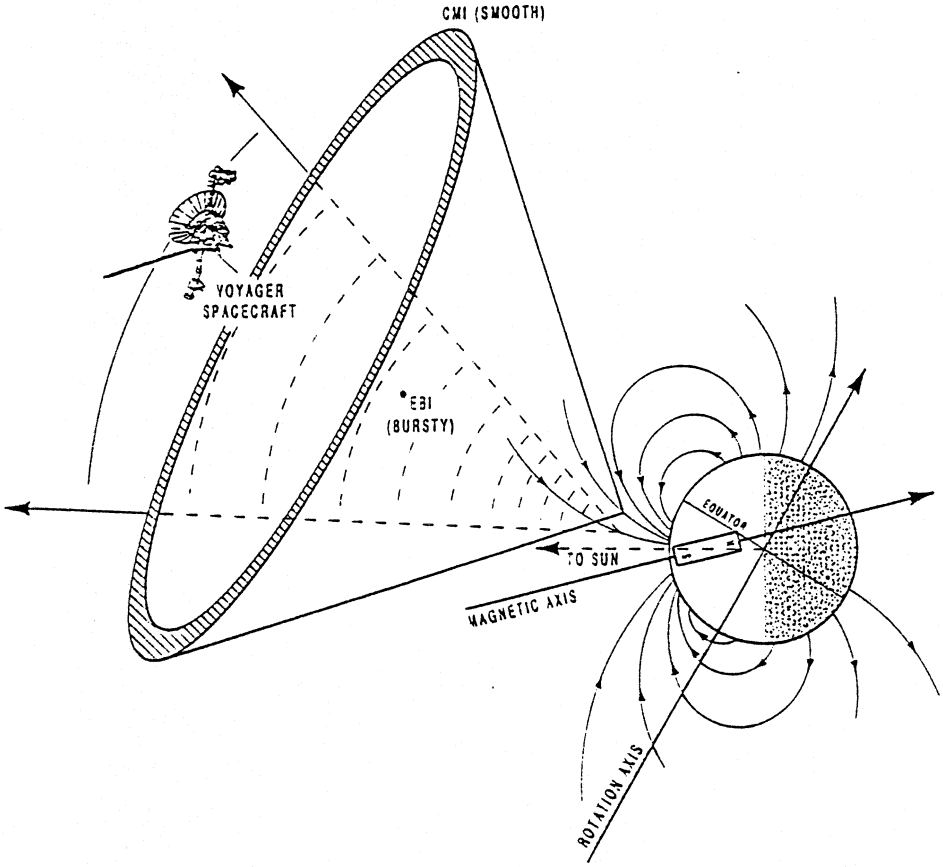

Figure 5: Schematic showing the radiation pattern in the proposed model. Radiation from the cyclotron maser emission (CMI) in a hollow cone generates the smooth emissions while the electromagnetic beam instability (EBI) generates radiation in a displaced solid cone to produce the bursty emissions.

exist adjacent to source regions of the cyclotron maser emission. In contrast, the smooth planetary emissions are believed to be generated by the cyclotron maser instability (CMI) which is presumably driven by the continuous injection of the energetic electrons and the subsequent development of loss–cone distributions.

These temperature anisotropic beams are unstable to a modified kinetic Weibel or electromagnetic beam instability. For $\omega_{pe}/\Omega_e \gtrsim 1$, most of the wave energy generated is LCP with frequencies below the cyclotron frequency and is therefore trapped. However, for $\omega_{pe}/\Omega_e \lesssim 1$ the dominant mode is RCP and freely propagating. The radiation in this regime is also bursty in nature due to the competition between different modes, particularly for small values of ω_{pe}/Ω_e. In addition, the electromagnetic beam instability is as efficient as the maser instability in converting particle energy into wave energy particularly when $\omega_{pe}/\Omega_e \gtrsim 0.4$.

Thus, the radiation from the electromagnetic beam instability (EBI) has many features similar to the observed bursty planetary emissions. Moreover, it strongly complements that of the maser radiation, both in the plasma conditions in which escaping radiation is generated and in the injection of the energetic electrons as it changes from continuous

to sporadic. This complementary nature provides a ready explanation for the apparent offsets in source location and spacecraft event time of the smooth and bursty emissions. In addition, Curran et al. [1990] have shown via a ray tracing study that for $\omega_{pe}/\Omega_e \lesssim 0.25$ and emission radiated in hollow cones at large wave normal angles, the source of Uranus broadband bursty emission is distinct from the b–smooth emission. No ray tracing studies of filled emission cones have yet been reported for either Uranus or Neptune.

The model presented here suggests a radiation pattern and source location similar to that shown in Figure 5, with the source regions of the two emissions approximately adjacent, as ω_{pe}/Ω_e and the characteristics of the electron injection vary across the polar regions. As a result of the different emission mechanisms and there source location, a spacecraft would be expected to see the two sides of the hollow cone of the smooth emissions followed by a single patch of bursty emission associated with emission from a filled cone, similar to the observations of Farrell and Calvert [1989].

While the above work provides a proof–in–principle of the importance of the EBI, more work needs to be carried out to fully determine the radiation pattern from the electromagnetic beam instability and its propagation through the magnetospheres of Neptune and Uranus.

Acknowledgements: This research was supported by NASA grants NAGW–2471, NAGW–2412 and NAGW–1936 and NSF grant ATM 91–96132 to Southwest Research Institute and by SWRI Internal Research grants 15–9668 and 15–9677. The simulations were performed on the CRAY Y–MP at the San Diego Supercomputing Center which is funded by the National Science Foundation.

References

Curran, D. B., J. D. Menietti, and H. K. Wong, Ray tracing of broadband bursty radio emissions from Uranus, *Geophys. Res. Lett.*, **17**, 109, 1990.

Farrell, W. M. and W. Calvert, The source location and beaming of broadband bursty radio emissions from Uranus, *J. Geophys. Res.*, **94**, 217, 1989.

Farrell, W. M., M. D. Desch, and M. L. Kaiser, Field–independent source localization of Neptune's radio bursts, *J. Geophys. Res.*, **95**, 19143, 1990.

Goldman, M. V. and D. Newman, Electromagnetic beam modes driven by anisotropic electron streams, *Phys. Rev. Lett.*, **58**, 1849, 1987.

Kaiser, M. L., M. D. Desch, and S. A. Curtis, The sources of Uranus' dominant nightside radio emissions, *J. Geophys. Res.*, **92**, 15169, 1987.

Ladreiter, H. P, Y. Leblanc, G. Rabl and H. O. Rucker, Emission characteristics and source location of smooth Neptunian kilometric radiation, *J. Geophys. Res.*, **96**, 19101, 1991.

Leblanc, Y., M. G. Aubier, A. Ortega–Molina, and A. Lecacheux, Overview of the Uranian radio emissions: Polarization and constraints on source locations, *J. Geophys. Res.*, **92**, 15125, 1987.

Menietti, J. D., H. K. Wong, D. A. Wah, and C. S. Lin, Source region of the smooth high frequency nightside Uranus kilometric radiation, *J. Geophys. Res.*, **95**, 51, 1990.

Menietti, J. D. and J. L. Burch, Particle acceleration in the auroral region as observed by DE–1, Proc. AGU Chapman Conference on Auroral Plasma Dynamics, October 21–25, 1991 in Minneapolis, MN.

Newman, D., R. M. Winglee, and M. V. Goldman, Theory and simulation of electromagnetic beam modes and whistlers, *Phys. Fluids*, **31**, 1515, 1988.

Pritchett, P. L., Electron–cyclotron maser instability in relativistic plasmas, *Phys. Fluids*, **29**, 2919, 1986.

Urrutia, J. M. and R. L. Stenzel, New electromagnetic mode in a non–Maxwellian high–beta plasma, *Phys. Rev. Lett.*, **53**, 1901, 1984.

Warwick, J. W., D. R. Evans, G. R. Peltzer, R. G. Peltzer, J. H. Romig, C. B. Sawyer, A. C. Riddle, A. E. Schweitzer, M. D. Desch, M. L. Kaiser, W. M. Farrell, T. D. Carr, I. de Pater, D. H. Staelin, S. Gulkis, R. L. Poyntner, A. Boischot, F. Genova, Y. Leblanc, A. Lecacheux, B. M. Pedersen, P. Zarka, Voyager planetary radio astronomy at Neptune, *Science*, **246**, 1498, 1989.

White, S. M., D. B. Melrose and G. A. Dulk, Electron cyclotron masers during solar flares, *Astrophys. J.*, **308**, 424, 1986.

Winglee, R. M. and G. A. Dulk, The electron–cyclotron maser instability as the source of solar type V continuum, *Astrophys. J.*, **310**, 432, 1986.

Wong, H. K. and M. L. Goldstein, A mechanism for bursty radio emission in planetary magnetospheres, *J. Geophys. Res.*, **17**, 2229, 1990.